

# DESIGN OF BEAM OPTICS FOR THE FCC-ee COLLIDER RING

K. Oide\*, K. Ohmi, D. Zhou, KEK, Tsukuba, Japan  
 U. Wienands, ANL, Argonne, Illinois, U.S.A.  
 A. Bogomyagkov, I. Koop, E. Levichev, P. Piminov,  
 D. Shatilov, D. Shwartz, S. Sinyatkin, BINP SB RAS, Novosibirsk, Russia  
 S. Aumon, M. Benedikt, H. Burkhardt,  
 A. Doblhammer, B. Haerer, B. Holzer, J.M. Jowett, L. Medina,  
 Y. Papaphilippou, J. Wenninger, F. Zimmermann†, CERN, Geneva, Switzerland  
 A. Blondel, M. Koratzinos, DPNC/Geneva University, Geneva, Switzerland  
 M. Boscolo, INFN/LNF, Frascati, Italy  
 M. Aiba, PSI, Villigen PSI, Switzerland  
 Y. Cai, M. Sullivan, SLAC, Menlo Park, California, U.S.A.

## Abstract

A design of beam optics is made for the FCC-ee double-ring  $e^+e^-$  collider. The main characteristics of the design are: 45 to 175 GeV beam energy, 100 km circumference with two interaction points (IPs) per ring, horizontal crossing angle of 30 mrad at the IP, and the crab-waist scheme with local chromaticity correction system. A so-called “tapering” of the magnets is applied, which scales all fields of magnets with the local beam energy to compensate the synchrotron radiation (SR) loss along the ring. An asymmetric layout near the interaction region suppresses the critical energy of SR incoming to the detector at the IP below 100 keV, while matching the geometry to the beam line of the FCC proton collider (FCC-hh) [1] as close as possible. Sufficient transverse/longitudinal dynamic apertures (DAs) have been obtained to assure the beam lifetime with beamstrahlung and top-up injection. The synchrotron radiation loss in all magnets as well as the IP solenoids with compensation are taken into account.

## REQUIREMENTS AND PARAMETERS

The FCC-ee is a double-ring collider to be installed in a common tunnel of  $\sim 100$  km circumference, as a potential first step before FCC-hh. The beam energy covers at least from Z-pole (45.6 GeV) to  $t\bar{t}$  (175 GeV). The design restricts the total synchrotron radiation power at 100 MW, thus the stored current per beam varies from 1.45 A at Z to 6.6 mA at  $t\bar{t}$ . This design assumes that the beam optics simply scale with the energy, except for the detector solenoid, which will be kept constant at all energies together with the compensation solenoids. A 30 mrad horizontal crossing angle with the crab-waist scheme is applied at each IP at all energies [2]. The SR of the incoming beam to the IP has been set below 100 keV at  $t\bar{t}$ , from dipoles upstream up to  $\sim 500$  m.

This collider ring must have enough DA to store the colliding beam, whose energy spread is drastically increased by the beamstrahlung, and to maintain the beam current considering the lifetime and the ability of the top-up injection.

In particular, the dynamic momentum acceptance must be larger than  $\pm 2\%$  at  $t\bar{t}$ . Similar acceptance would be required at lower energies, if top-up injection in longitudinal phase space is needed.

Table 1: Machine Parameters of FCC-ee. The beam optics simply scales with beam energy. The values in parenthesis correspond to optional cases.

Circumference [km]	99.984	
IPs / ring	2	
Crossing angle at IP [mrad]	30	
Solenoids at IP [T]	$\pm 2$	
$l^*$ [m]	2.2	
Local chrom. correction	y-plane with crab sexts	
Arc cell	FODO, $90^\circ/90^\circ$	
mom. compaction [ $10^{-6}$ ]	7.0	
$\nu_x/\nu_y$	387.08/387.14	
Arc sextupoles	292 pairs	
RF frequency [MHz]	400	
Beam energy [GeV]	45.6	175
SR energy loss/turn [GeV]	0.0346	7.47
Current/beam [mA]	1450	6.6
Bunches/ring	30180 (91500)	81
Total SR power [MW]	100.3	98.6
Horizontal emittance [nm]	0.86	1.26
$\epsilon_y/\epsilon_x$ w/beam-beam [%]	0.6	0.2
$\beta_x^*$ [m]	0.5 (1)	1 (0.5)
$\beta_y^*$ [mm]	1 (2)	2 (1)
Energy spread by SR [%]	0.038	0.141
Bunch length by SR [mm]	2.8 <sup>a</sup>	2.4 <sup>b</sup>
$\nu_z$	-0.0158 <sup>a</sup>	-0.0657 <sup>b</sup>
Luminosity/IP [ $10^{34}/\text{cm}^2\text{s}$ ]	210 (90)	1.3 (1.5)

<sup>a</sup> for  $V_c = 78$  MV

<sup>b</sup> for  $V_c = 9.04$  GV

Table 1 shows the machine parameters. The optics simply scales with the energy. The minimum achievable  $\beta_{x,y}^*$  are (0.5 m, 1 mm) at all energies, and they should be chosen to maximize the luminosity performance at each energy.

## LAYOUT

The schematic layout of the FCC-ee rings is shown in Fig. 1. The basic geometry just follows the current layout of the FCC-hh ring. The  $e^+e^-$  rings are placed side by side. In the arc sections, the center of  $e^+e^-$  rings is exactly placed on the center of the hh-rings, while offsets by about 1 m in the

\* Katsunobu.Oide@kek.jp

† Presenter

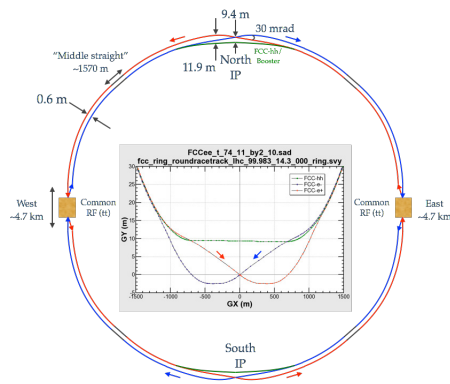


Figure 1: Layout of the FCC-ee collider rings. Two IPs are located at the North and South straight sections, and the RFs are placed on East and West. Short intermediate straight sections are in the middle of each arc. Beams cross over in the RF section. The south IP is enlarged in the middle figure. The green line indicates the FCC-hh beam line or the booster synchrotron for FCC-ee.

straight sections except for the interaction region (IR). The layout in the IR is greatly constrained by the requirement on the incoming synchrotron radiation. As the incoming beam cannot be bent strongly to reduce the radiation, and generating a certain amount of the crossing angle at the IP, the beam must come from the inner ring to the IP, bending stronger after the IP to merge. Thus the IP of the  $e^+e^-$  rings must displace outside relative to the hh-beam. The size of the displacement of the IP depends on the limit of the critical energy to the IP. In the design shown in Fig. 1 has such a displacement of 9.4 m. The  $e^+e^-$  beams separate from the hh beam line reaching the maximum deviation 11.9 m at around  $\pm 400$  m from the IP. The outgoing beam returns to the hh beam line at around  $\pm 1.2$  km from the IP, then a wide tunnel or double tunnels are needed for this region. These sizes of the separations can be reduced if the criteria for the SR is relaxed, as shown in a design [3]. The shift of the IP is suitable to install the booster synchrotron along the hh beam line to bypass the  $e^+e^-$  detector.

At each IP, the beam must come from the inside. Thus the beams must cross over somewhere between the IPs. This is naturally done by making the RF cavities common to both beams, especially in the case of  $t\bar{t}$ . If only a half of each ring is filled by bunches, each beam passes the cavities without seeing the other beam. As the bunches per ring (80 @  $t\bar{t}$ ), are much smaller than the bucket number ( $\sim 133400$ ), the half filling does not cause an issue. Moreover, the RF cavities are loaded with the two beams alternatively, and an issue of transient loading is small. At lower energies, such a common RF is not necessary, and a simple crossing without interaction can be applied.

## OPTICS

### Arc

The arc optics basically consists of  $90^\circ/90^\circ$  FODO cells. Two noninterleaved families of sextupole pairs, having a  $-I$  transformation between sextupoles, are placed in a 5 FODO

supercell. The number of cells is determined to achieve the equilibrium horizontal emittance, resulting in 292 independent sextupole pairs in a half ring. So far we have assumed a complete period 2 periodicity of the ring optics. The length of quadrupoles must be chosen considering the power consumption as well as the effect of the synchrotron radiation on the DA as discussed later. There is a possibility to use a combined function dipole for the arc cell to reduce the number of cells in the arc, keeping the horizontal emittance. A preliminary study shows a reduction of number of cells by about 30% by introducing a field gradient in the dipoles to change the longitudinal damping partition from 2.0 to 0.6.

### IR

Figure 2 shows the optics of the IR, corresponding to  $\beta_{x,y}^* = (1 \text{ m}, 2 \text{ mm})$ . It has a local chromaticity correction system (LCCS) only in the vertical plane at each side of the IP. Sextupoles are paired at each side, but the inner sextupoles close to the IP have nonzero horizontal dispersion. The outer sextupoles not only cancel the geometrical nonlinearity of the inner ones, but also generate crab-waist at the IP by choosing the phase advances between the IP as  $\Delta\psi_{x,y} = (2\pi, 2.5\pi)$ . This incorporation of the crab sextupole into the LCCS saves space and the number of optical components.

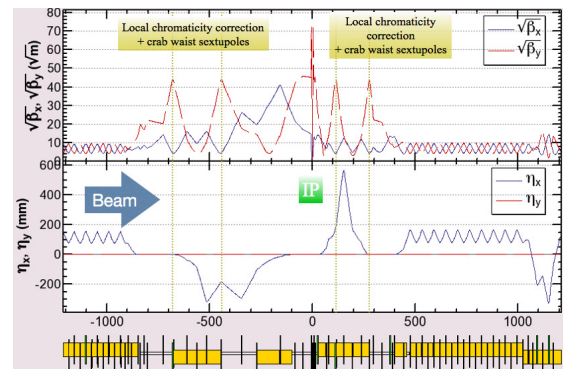


Figure 2: The beam optics of the IR of FCC-ee. The optics is asymmetric, and beam comes from the left to the right in this figure. Dipoles are shown by yellow boxes. Sextupoles for the LCCS are located at the golden vertical lines. The outer ones also work as crab sextupoles.

The optics at the interaction region [4] is basically separated for two beams. There is no common quadrupoles in the IR. The solenoids are common, but they are locally compensated with counter solenoids to cancel  $\int B_z dz$  between the IP and the face of the final quadrupole. No vertical orbit, vertical dispersion,  $x$ - $y$  couplings are leaked to the outside for any particle at any energy. So far we have assumed such a perfect compensation. The final quadrupoles have a field gradient of 100 T/m, and the detector field is shielded on the quadrupoles by another anti-solenoid.

The critical energy from the dipoles up to 500 m upstream of the IP are set below 100 keV at  $t\bar{t}$ . There is no dipole magnet before the IP up to 100 m.

### RF Section and Other Straight Sections

The RF sections are located the East & West straight sections in Fig. 1. At  $t\bar{t}$ , an acceleration voltage 4.5 GV is needed within about 1 km. A combination of electrostatic separator and a dipole magnets deflects only the outgoing beam to avoid the synchrotron radiation toward the RF cavities. The quadrupoles within the RF section are common for both beams, but are still compatible to the tapering scheme, if their strengths are symmetrically chosen.

The usage of the intermediate straight sections in the middle of the arc has not been determined. Some of them can be used for injection, dump, and collimation, etc. The current optics for them are just tentative.

### DYNAMIC APERTURE

Dynamic aperture has been estimated using SAD [5] for this optics, considering a number of effects listed in Table 2. Among them, the synchrotron radiation plays essential roles. While the radiation in the dipole improves the aperture especially at  $t\bar{t}$  by the strong damping, radiation in quadrupoles for particles with large betatron amplitudes reduces the aperture, by inducing a synchrotron motion through the radiation loss in the quadrupoles. This effect is mostly noticeable for arc horizontal quadrupoles, thus the length of the arc quadrupole must be sufficiently long. The final quadrupole has the similar effect on the vertical motion due to the large  $\beta_y$  and the strong field gradient at the quadrupole.

Table 2: Effects Taken into Account in the Estimation of the Dynamic Aperture

Effects	Included?	Significance at $t\bar{t}$
Synchrotron motion	Yes	<b>Essential</b>
Radiation in dipoles	Yes (no fluctuation)	<b>Essential</b> – improves the aperture
Radiation in quadrupoles	Yes (no fluctuation)	<b>Essential</b> – reduces the aperture
Tapering	Yes	<b>Essential</b>
Crab waist	Yes	Aperture is reduced by ~ 20%
Solenoids	Yes	minimal, if locally compensated
Maxwellian fringes	Yes	small
Kinematical terms	Yes	small
Beam-beam effects	Yes (strong-weak)	affects the lifetime [6]
Higher order fields/errors/misalignn	No	<b>Essential</b> , development of correction/tuning scheme is necessary

The DA has been optimized by searching sextupole settings by particle tracking with the downhill simplex method scripted in SAD. Figure 3 shows a result of such an optimization. The resulting DA satisfies the requirements for both beam-beam and injection, at least without errors and misalignments, even including the strong-weak beam-beam interactions. The optimization must be done for each setting of  $\beta_{x,y}^*$ , tunes, and the beam energy (radiation).

So far a very large number of sextupole families have been used in the optimization, it has not been verified whether

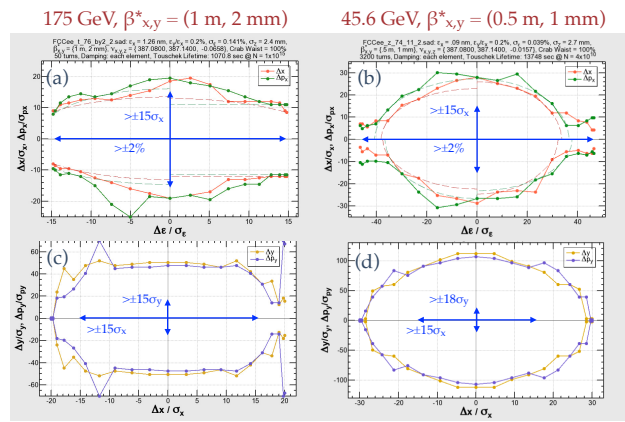


Figure 3: Dynamic apertures after optimization of sextupoles via particle tracking. (a, c):  $\beta_{x,y}^* = (1 \text{ m}, 2 \text{ mm})$ , 50 turns at  $t\bar{t}$ , (b, d):  $\beta_{x,y}^* = (0.5 \text{ m}, 1 \text{ mm})$ , 3,200 turns at Z. (a, b): z-x plane, (c, d): x-y plane. The blue lines show the required DAs for the beam-beam and the top-up injection.

these numbers are really necessary. Solutions with fewer families have been also investigated [3, 7].

### ISSUES

There are several issues remaining to be addressed at least:

- Development of correction/tuning schemes on the emittance and the dynamic aperture to mitigate the possible higher-order fields, machine errors, and misalignments.
- Refinement of the IR region collaborating with the machine-detector interface group.
- Iterations considering hardware designs of the RF, beam pipes, and magnets.
- Development of the injection scheme and necessary optics.
- Exploring a possibility for 4 IPs per ring.

### ACKNOWLEDGEMENT

The authors thank D. Schulte for providing information on FCC-hh. Also thank R. Calaga, C. Cook, S. Fartoukh, P. Janot, E. Jensen, R. Kersevan, A. Milanese, P. Raimondi, J. Seeman, G. Stupakov, R. Tomas for useful discussions and suggestions.

### REFERENCES

- [1] A. Chancé, *et al*, Proc. IPAC'16, TUPMW020.
- [2] A. Bogomyagkov, E. Levichev, D. Shatilov, Phys. Rev. ST Accel. Beams, vol. 17, p. 041004, 2014.
- [3] A. Bogomyagkov, *et al*, Proc. IPAC'16, THPOR019.
- [4] M. Koratzinos, *et al*, Proc. IPAC'16, TUPOR023.
- [5] <http://acc-physics.kek.jp/SAD/index.html>
- [6] D. Zhou, presentation at FCC Week 2016, April 2016, Rome (2016).
- [7] B. Haerer, *et al*, Proc. IPAC'16, SUPSS048.